Supporting Information

Remarkable 980 nm circularly polarized luminescence from dinuclear Yb(III)-helicates with *D_4* symmetry

Lingli Wang, Zhiwei Yao, Wenru Huang, Ting Gao, Pengfei Yan, Yanyan Zhou* and Hongfeng Li*

School of Chemistry and Materials Science, Key Laboratory of Functional Inorganic Material Chemistry, Ministry of Education Heilongjiang University 74 Xuefu Road, Harbin 150080, China

*E-mail: lihongfeng@hlju.edu.cn; zhouyanyan@hlju.edu.cn

Table of Contents

1. Experimental section

1.1 Materials and measurements

(R)-(+)-1,1'-Bi-2-naphthol, (S)-(-)-1,1'-Bi-2-naphthol, 2-Acethyl-5-bromothiphene and $Ln(OTf)_3$ salts (Ln = Yb and Gd) were purchased from Chembee Chemical Reagent Co., Ltd. (China); other chemicals and solvents are of analytical reagent grade. The ^1H NMR, ^{13}C NMR, ^{19}F NMR and ^1H DOSY spectra were recorded with a Bruker AVANCE III 400 MHz spectrometers, the ^{19}F NMR chemical shifts are referenced to trifluoroacetic acid (TFA) and the ^1H NMR chemical shifts are in ppm relative to tetramethylsilane (TMS): $CDCl_3$ (7.26 ppm for ^1H), THF-d_8 (1.72 ppm, 3.58 ppm for ^1H, 66.60 ppm, 24.39 ppm for ^{13}C). Electrospray time-of-flight (ESI-TOF) mass spectra were recorded using a Bruker maXis mass spectrometer.

Single crystal X-ray crystal data of $Yb_2(S\text{-}BTHP)_4$ was recorded on a Xcalibur, Eos, Gemini diffractometer with Mo Ka radiation ($\lambda = 0.71073$ Å). The structure was solved by direct methods and refined on F^2 by full-matrix least-squares using the SHELXTL-2014 program.

UV-vis spectra were recorded on a Perkin-Elmer Lambda 25 spectrometer. The CD experiments were performed on an Olis DM245 spectrofluorimeter, and the CPL experiments were performed on NIR CPL SOLO spectrophotometer with Hamamatsu detector H10330C and QWP (Quarter Wave Plate). Photoluminescence spectra containing the emission, excitation and luminescence lifetime measurements were recorded on an Edinburgh FLS 980 spectrophotometer. The luminescence quantum yields of the Yb(III) complexes were measured using $[Yb(TTA)_3(H_2O)_2]$ as the reference ($\Phi = 0.35\%$ in toluene), and were calculated according to the well-known eqn. S1:

$$\Phi_{overall} = \frac{n^2 A_{ref} I}{{n_{ref}}^2 A I_{ref}} \qquad (S1)$$

Where n, A, and I denote the refractive index of solvent, the absorbance at the excitation wavelength, and the area of the emission spectrum respectively. Φ_{ref} represents the quantum yield of the $[Yb(TTA)_3(H_2O)_2]$ in toluene. The subscript ref denotes the reference, and the absence of a subscript implies an unknown sample. The estimated errors are ±10% for the quantum yields and ±5% for the lifetime determinations.

In luminescent lanthanide complexes, the total luminescence quantum yield (Φ_{tot}) of the complexes can be described by eqn. S2:

$$\Phi_{tot} = \eta_{ET}\Phi_{Ln} \qquad (S2)$$

The intrinsic quantum yields of Yb(III) ion luminescence could be estimated using the eqn. S3, after the calculation of the radiative lifetime (τ_{rad}) from the absorption spectra of Yb(III) ion in complexes (Figure. S28) with a modified Einstein equation (eqn. S4):

$$\Phi_{Ln} = \frac{k_r}{k_r + k_{nr}} = \frac{\tau_{obs}}{\tau_{rad}} \qquad (S3)$$

$$\frac{1}{\tau_{rad}} = k_r = 2303 \times \frac{8\pi c n^2 \tilde{v}_m^2 (2J+1)}{N_A(2J'+1)} \int \varepsilon(\tilde{v}) d\tilde{v} \qquad (S4)$$

$$\tilde{v}_m = \frac{\int \tilde{v} \cdot \varepsilon(\tilde{v}) d\tilde{v}}{\int \varepsilon(\tilde{v}) d\tilde{v}}$$

Where, N_A is Avogadro's number, c is the speed of light in centimeters per second, J and J' are the quantum numbers for the ground and excited states, respectively. $\int(\tilde{v})d\tilde{v}$ is the integrated spectrum of the f-f transition, $\tilde{\mathrm{V}}_{\mathrm{m}}$ is the barycenter of the transition, and n = 1.465 for THF solution.

1.2 Characterization

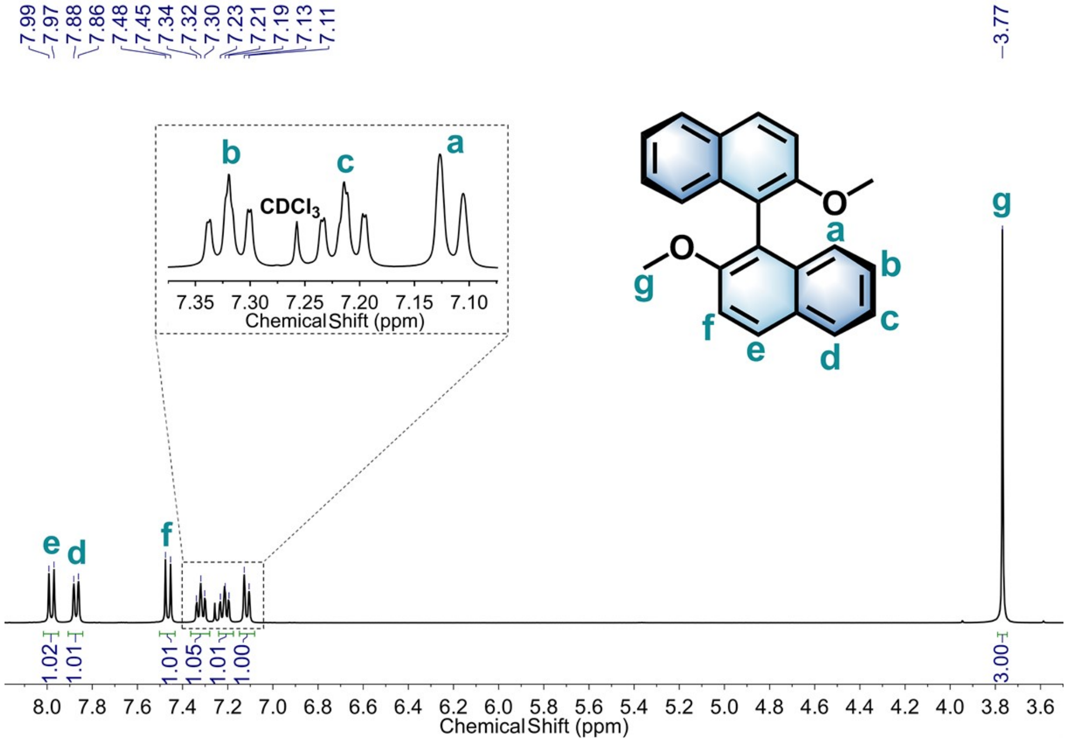

Figure S1. ^{1}H NMR spectrum (400 MHz, 298 K, CDCl$_3$) of S-**1**.

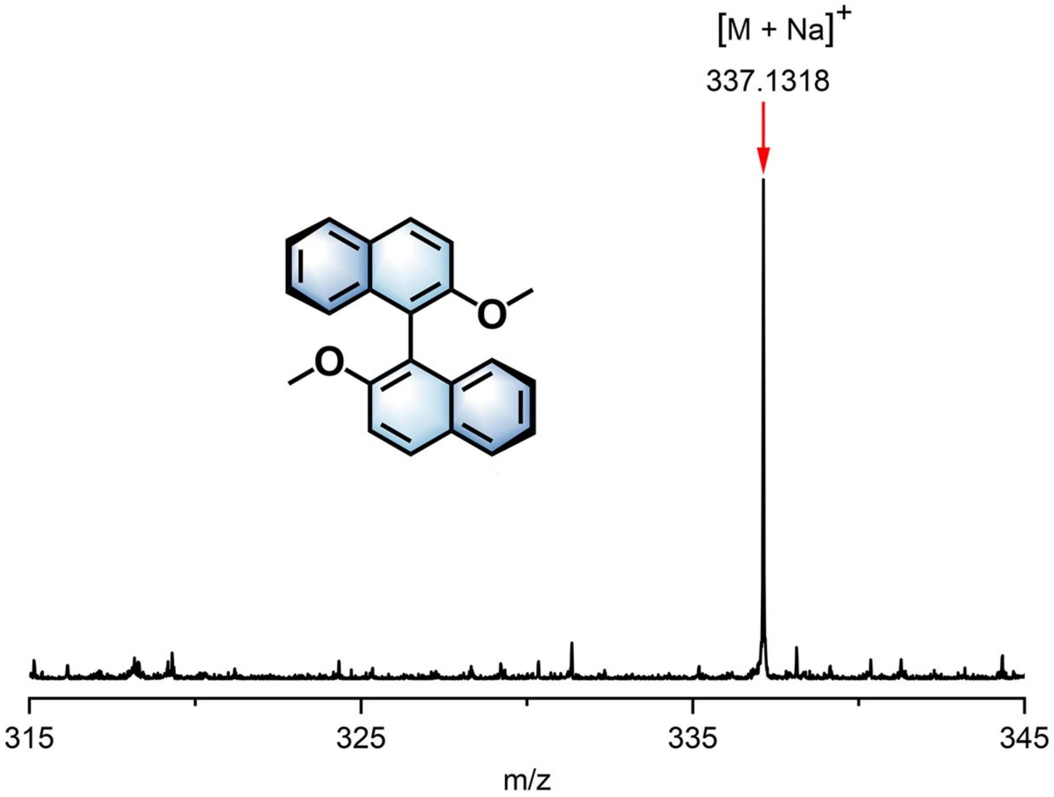

Figure S2. ESI-MS spectrum of S-**1**.

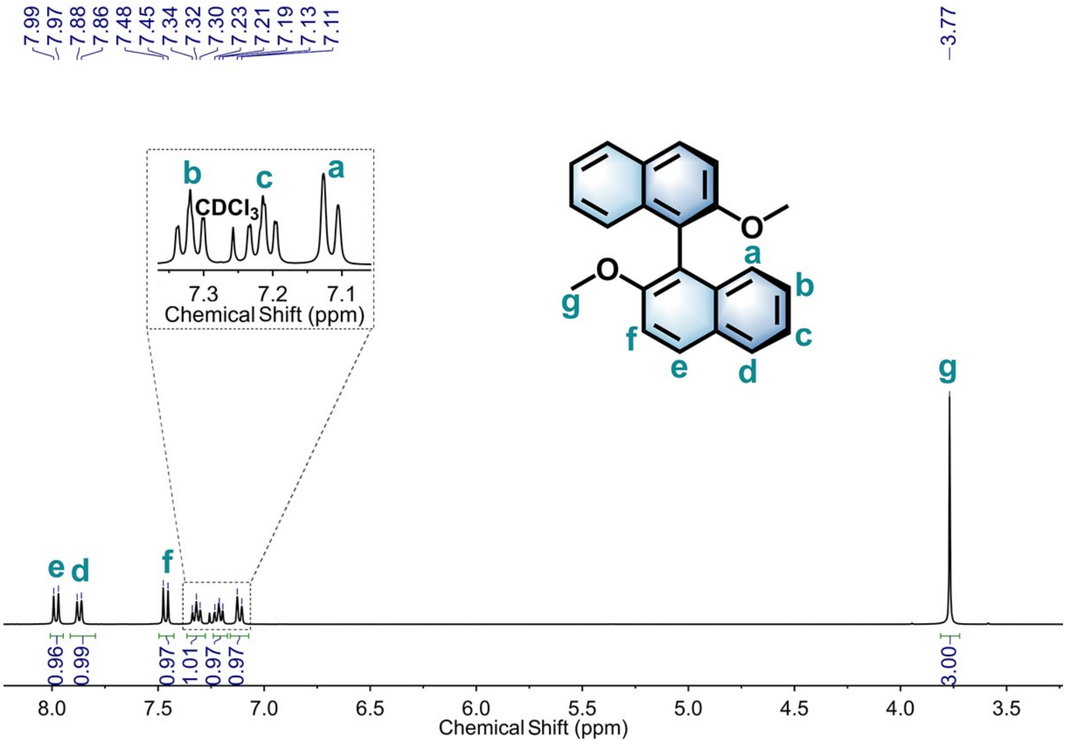

Figure S3. ^{1}H NMR spectrum (400 MHz, 298 K, CDCl$_3$) of R-**1**.

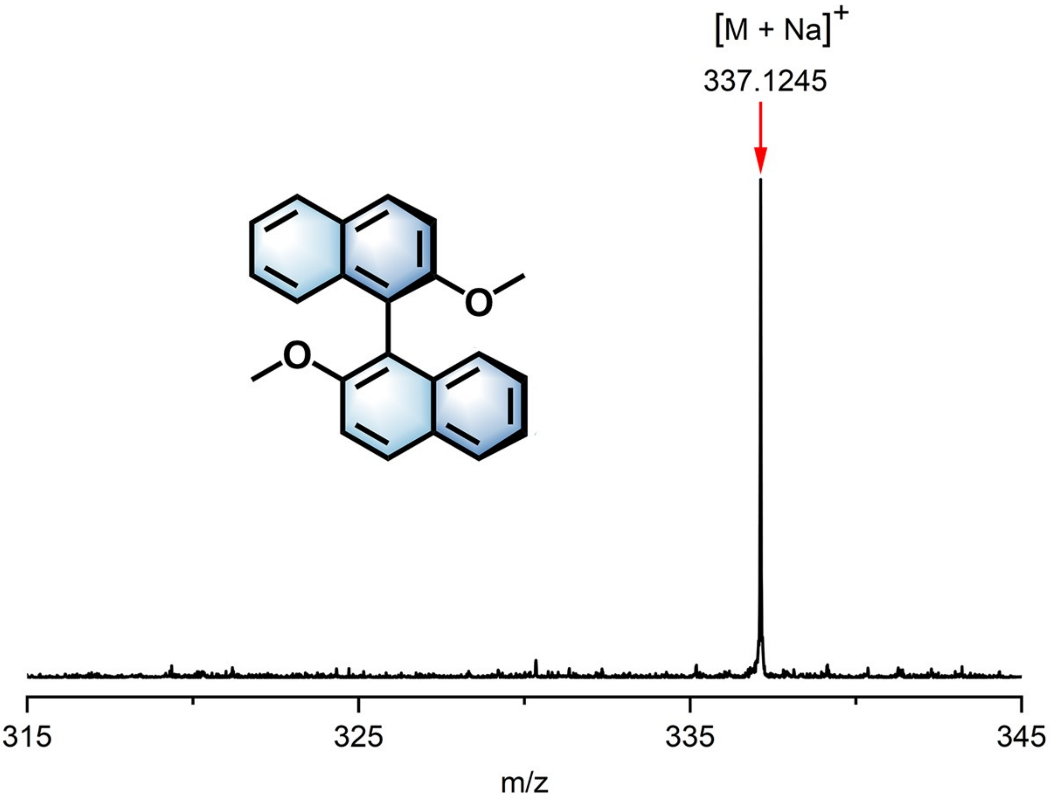

Figure S4. ESI-MS spectrum of R-**1**.

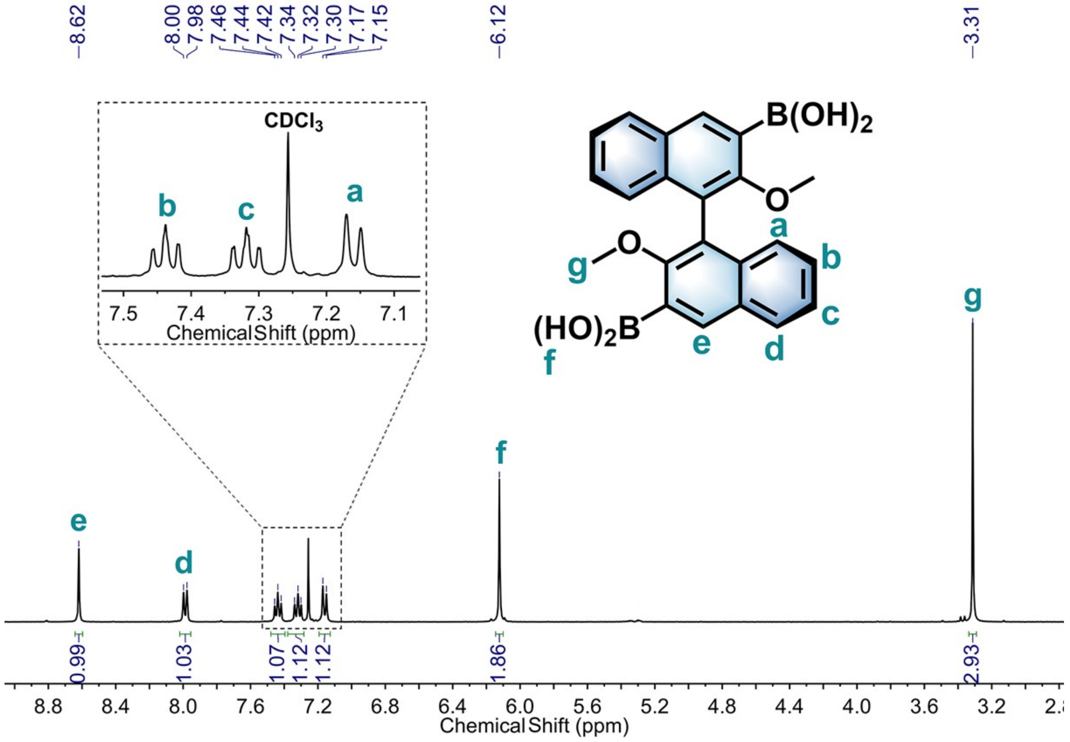

Figure S5. ^{1}H NMR spectrum (400 MHz, 298 K, $CDCl_3$) of S-**2**.

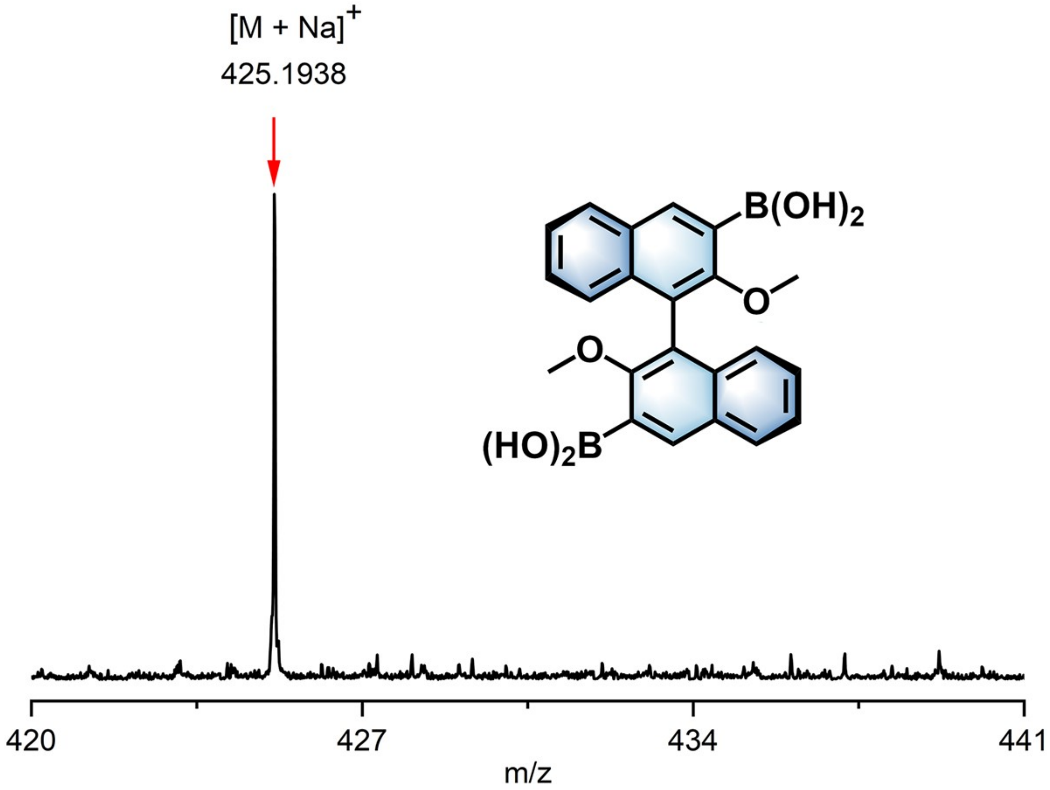

Figure S6. ESI-MS spectrum of S-**2**.

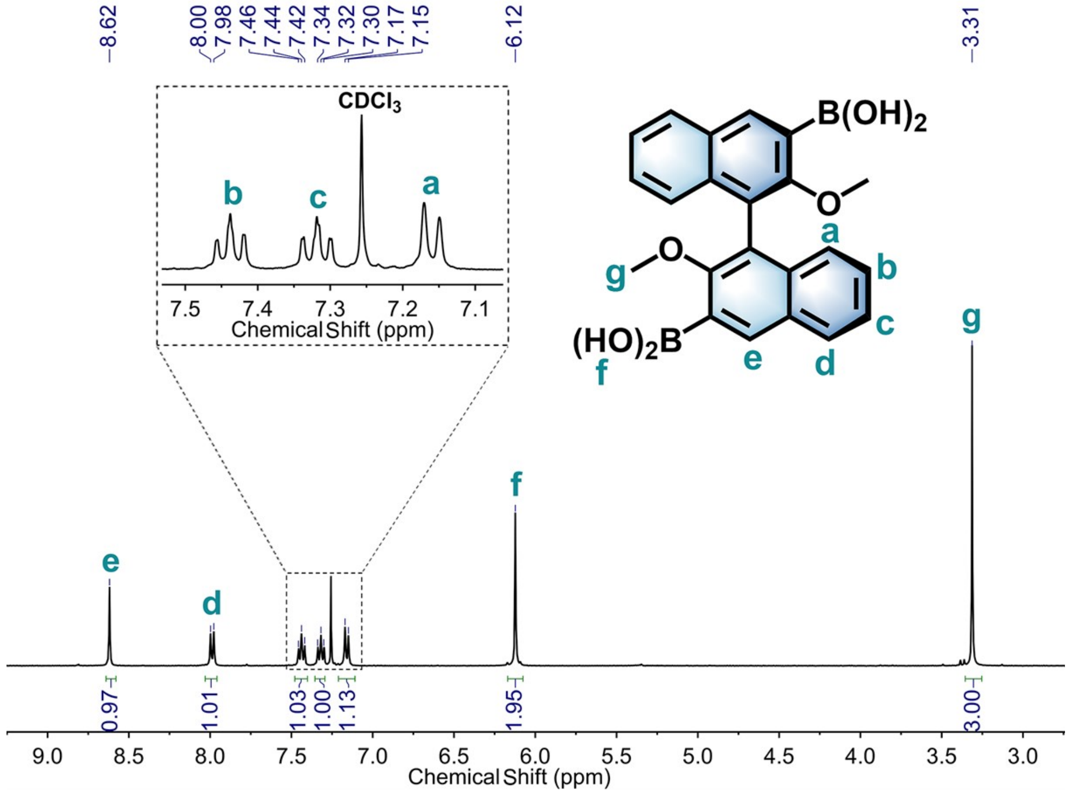

Figure S7. ^{1}H NMR spectrum (400 MHz, 298 K, CDCl$_3$) of R-**2**.

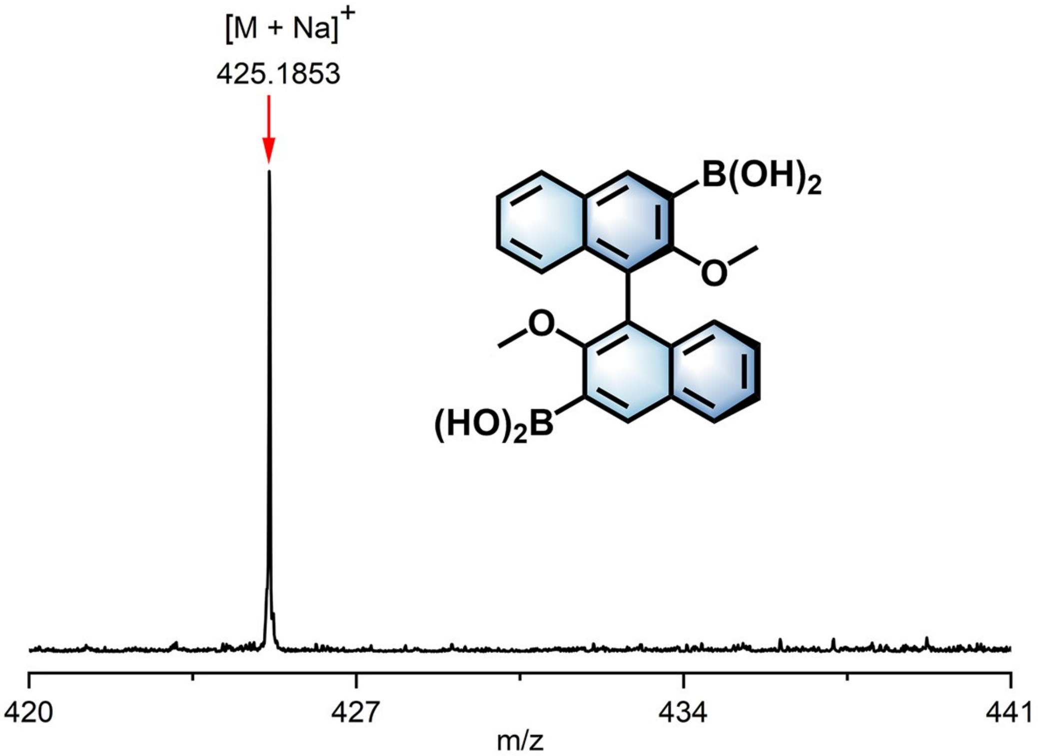

Figure S8. ESI-MS spectrum of R-**2**.

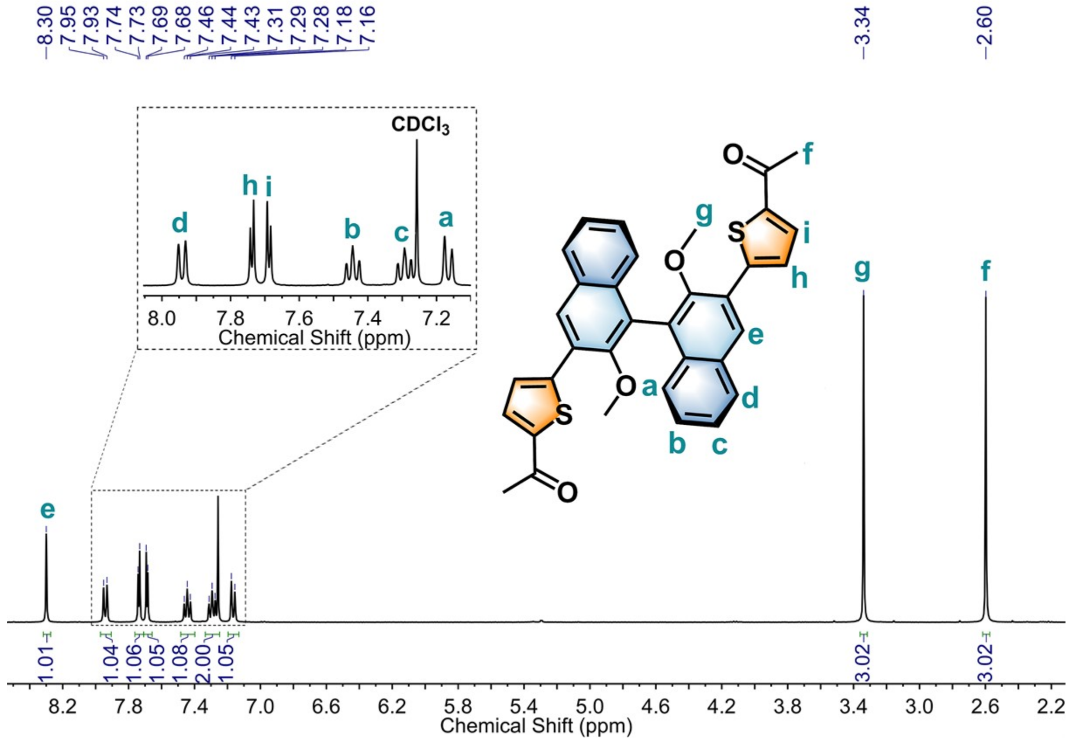

Figure S9. ^1H NMR spectrum (400 MHz, 298 K, $CDCl_3$) of S-**3**.

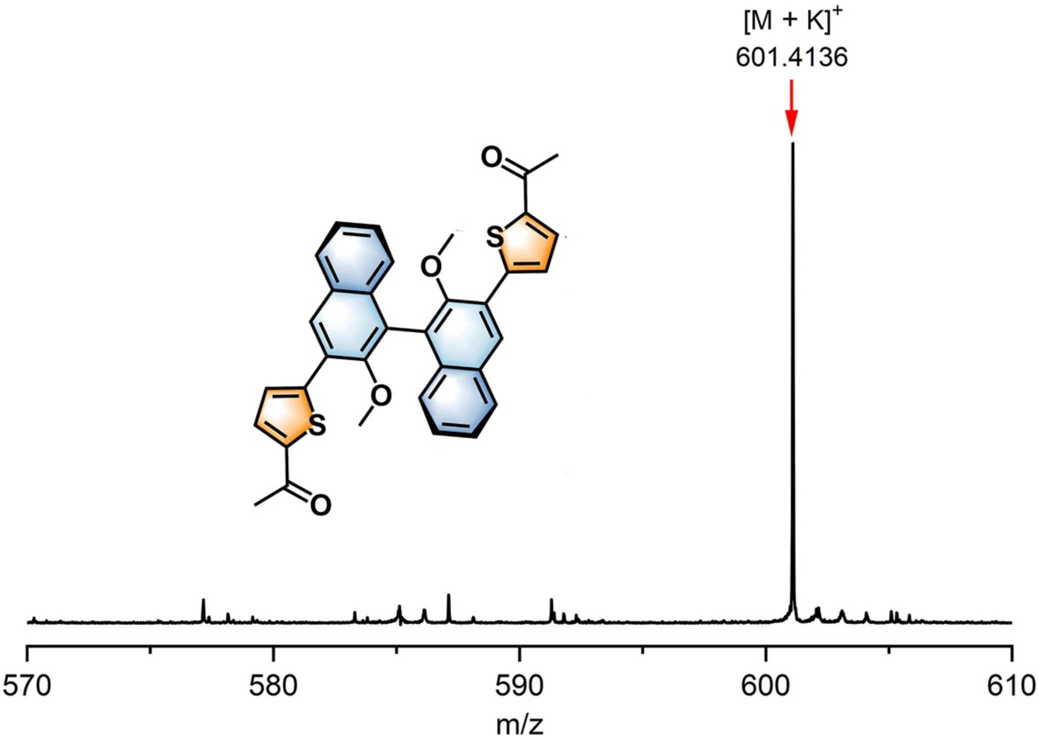

Figure S10. ESI-MS spectrum of S-**3**.

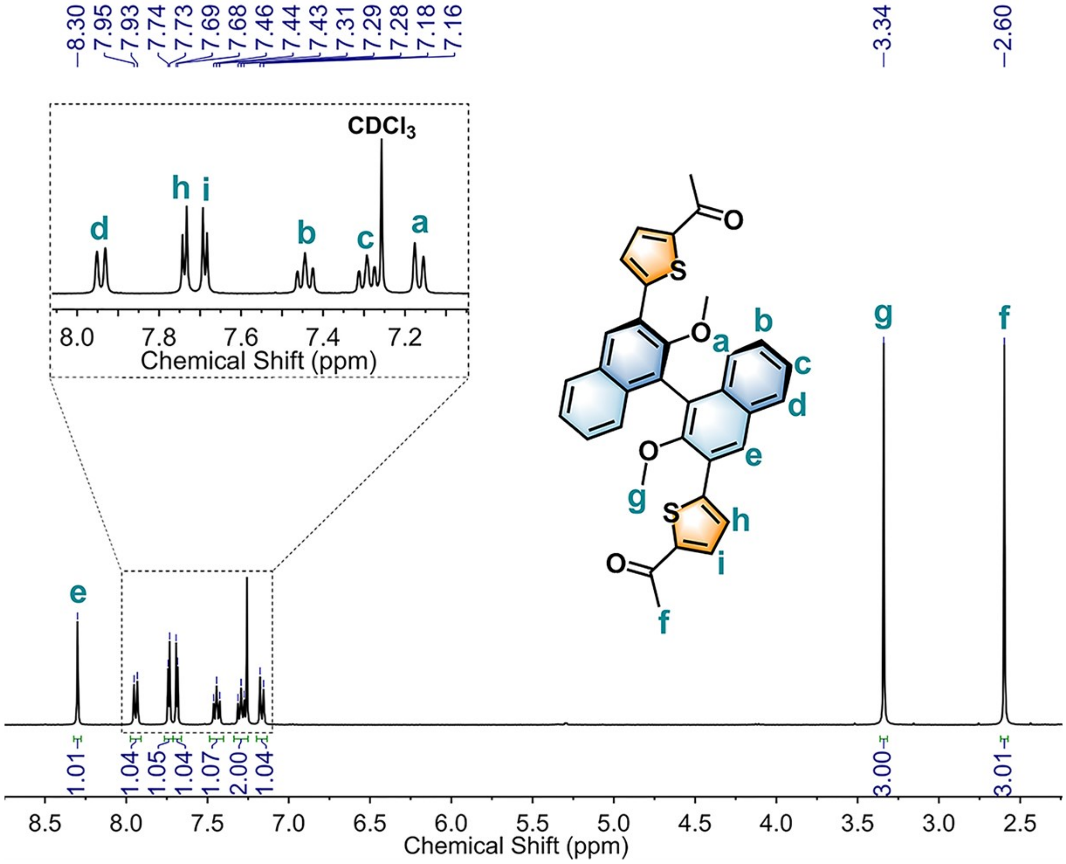

Figure S11. ^{1}H NMR spectrum (400 MHz, 298 K, CDCl$_3$) of R-**3**.

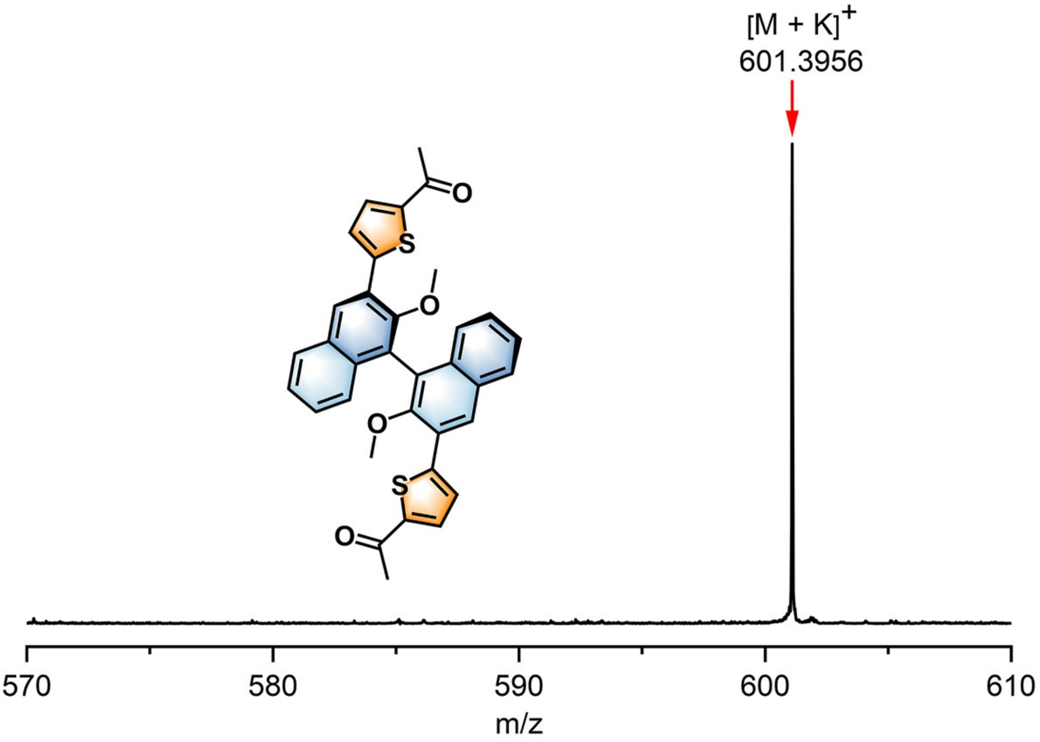

Figure S12. ESI-MS spectrum of R-**3**.

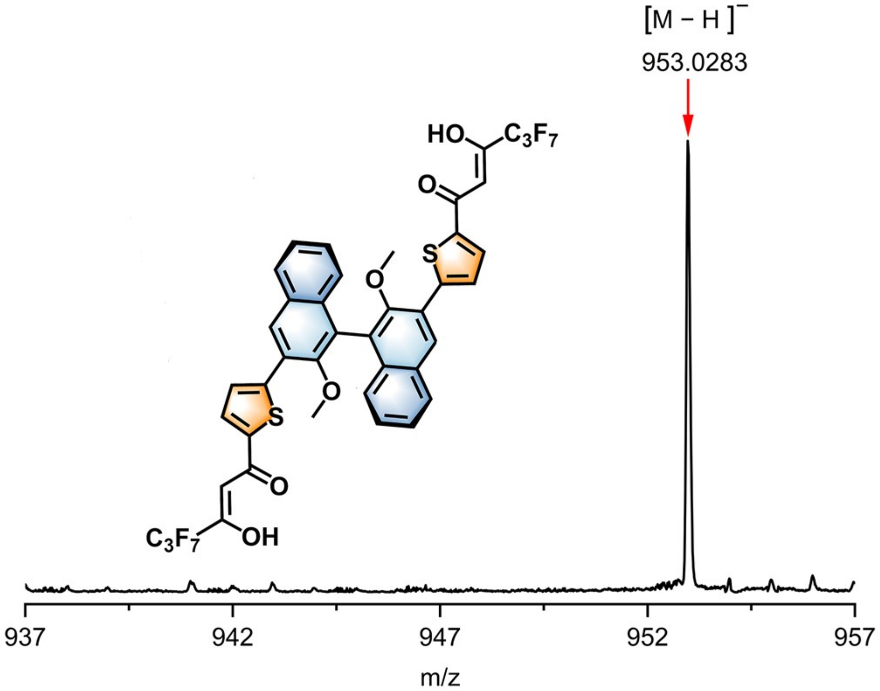

Figure S13. ESI-MS spectrum of S-BTHP.

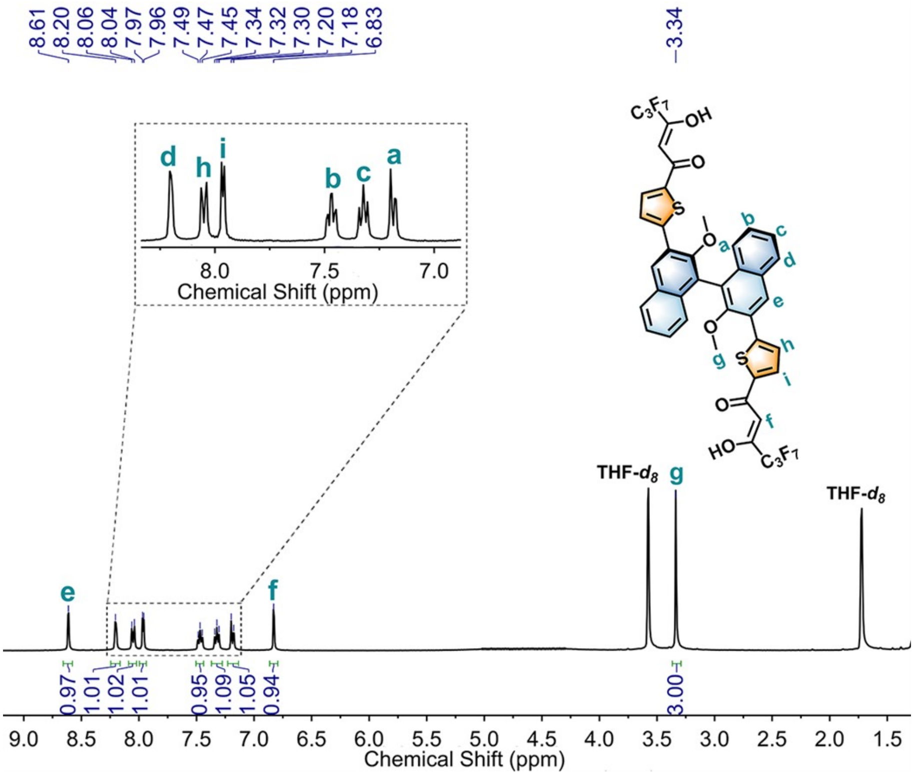

Figure S14. ^{1}H NMR spectrum (400 MHz, 298 K, THF-d_8) of R-BTHP.

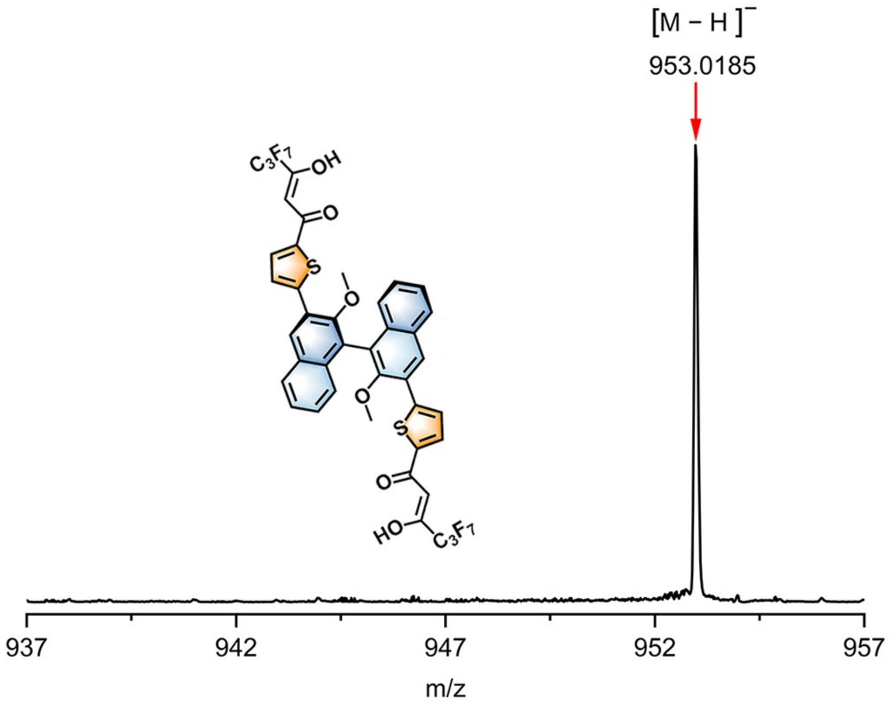

Figure S15. ESI-MS spectrum of R-BTHP.

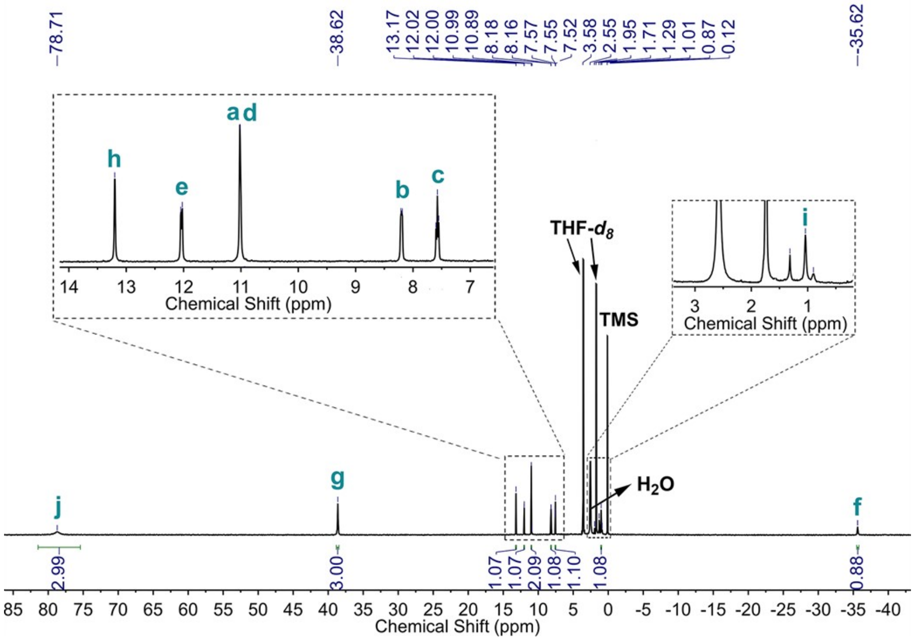

Figure S16. ^{1}H NMR spectrum (400 MHz, 298 K, THF-d_8) of Yb_2(R-BTHP)$_4$.

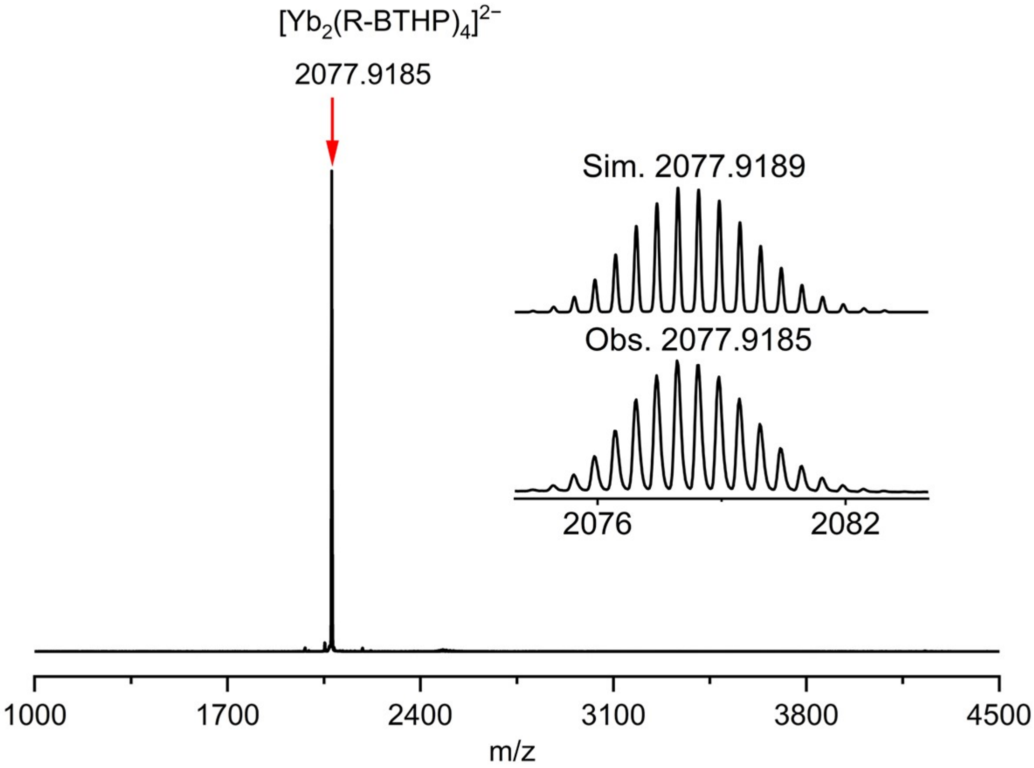

Figure S17. ESI-MS spectrum of Yb_2(R-BTHP)$_4$.

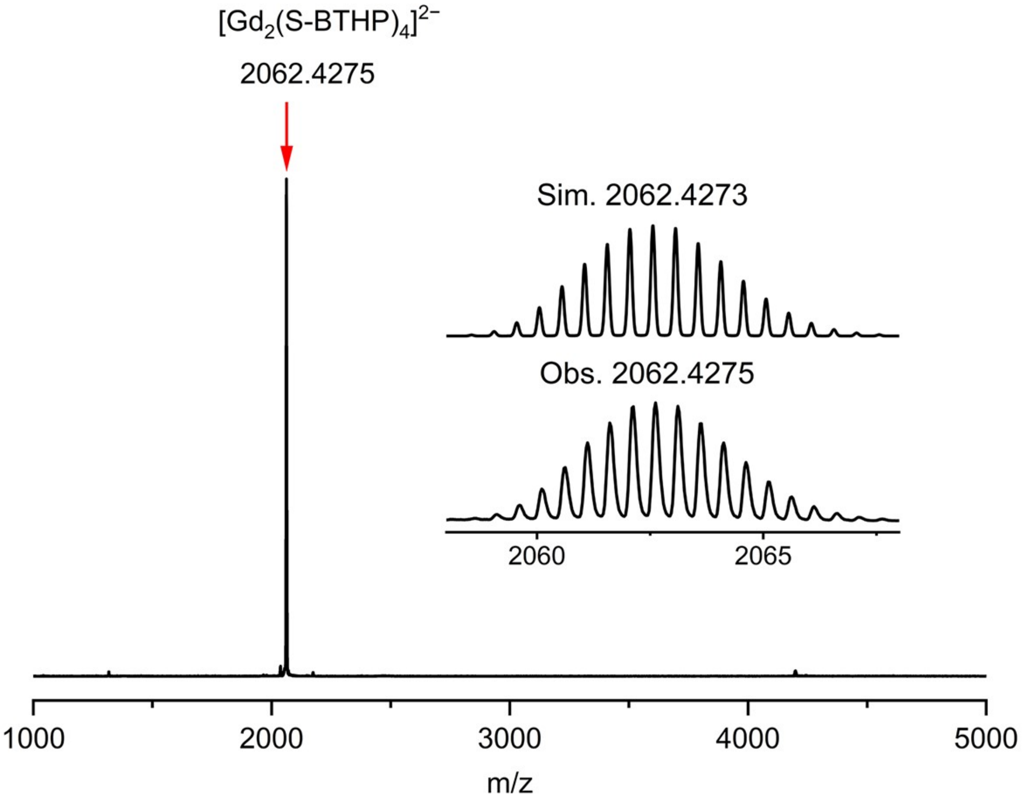

Figure S18. ESI-MS spectrum of Gd$_2$(S-BTHP)$_4$.

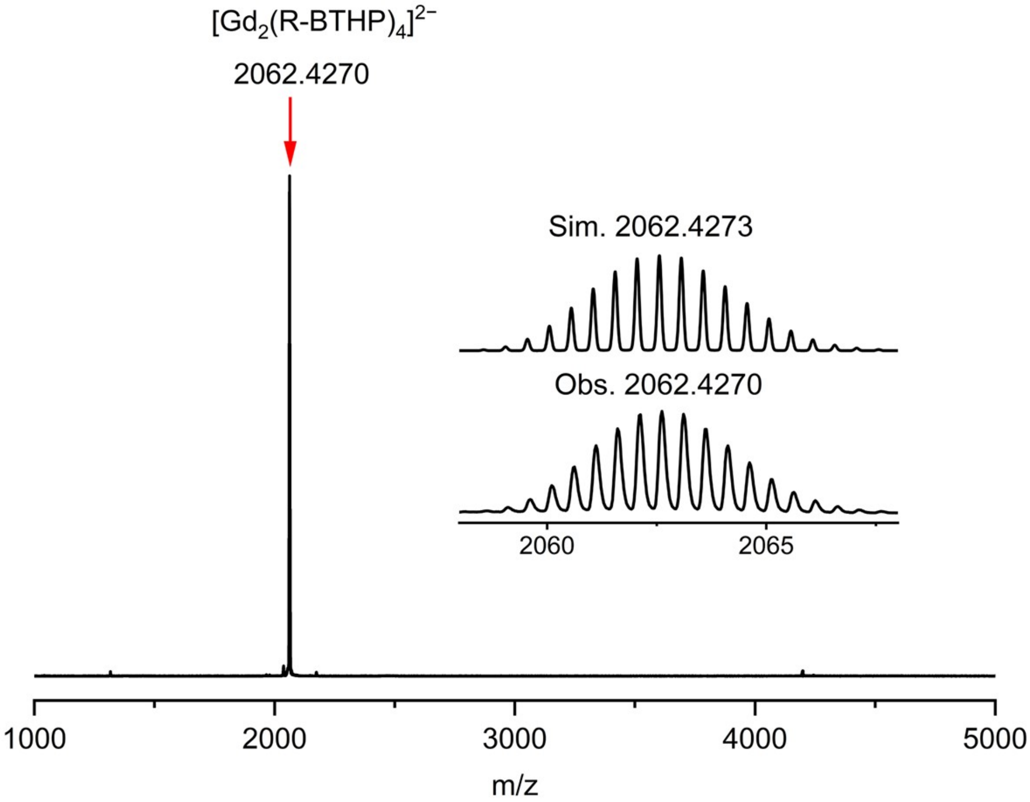

Figure S19. ESI-MS spectrum of Gd$_2$(R-BTHP)$_4$.

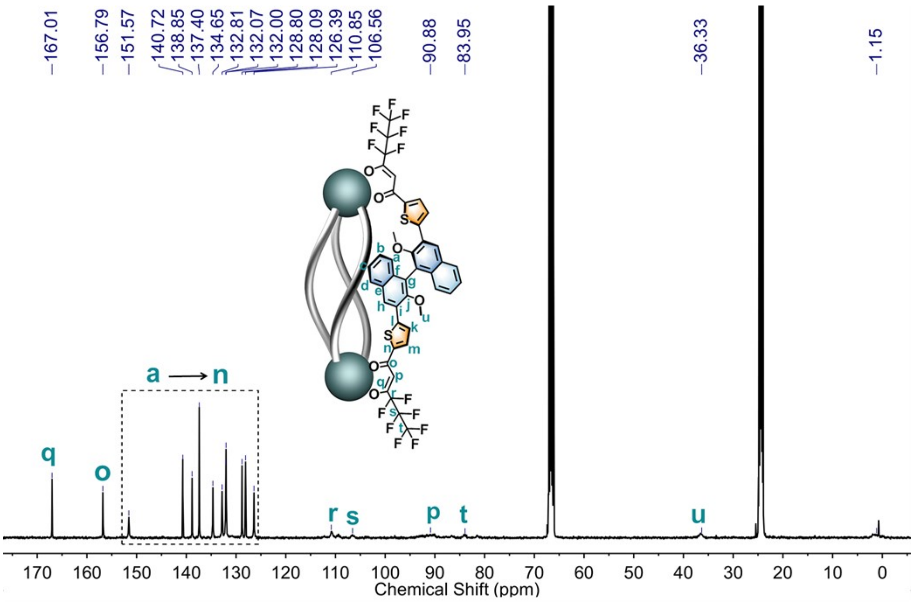

Figure 20. ^{13}C NMR spectrum (101 MHz, 298 K) of $Yb_2(S\text{-}BTHP)_4$ in THF-d_8.

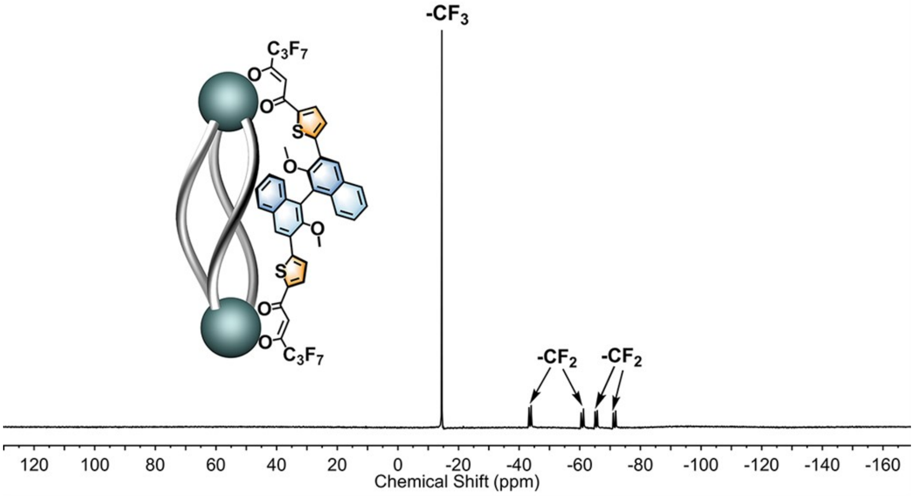

Figure S21. ^{19}F NMR spectrum (376 MHz, 298 K) of $Yb_2(S\text{-}BTHP)_4$ in THF-d_8.

2. Optical/chiroptical properties

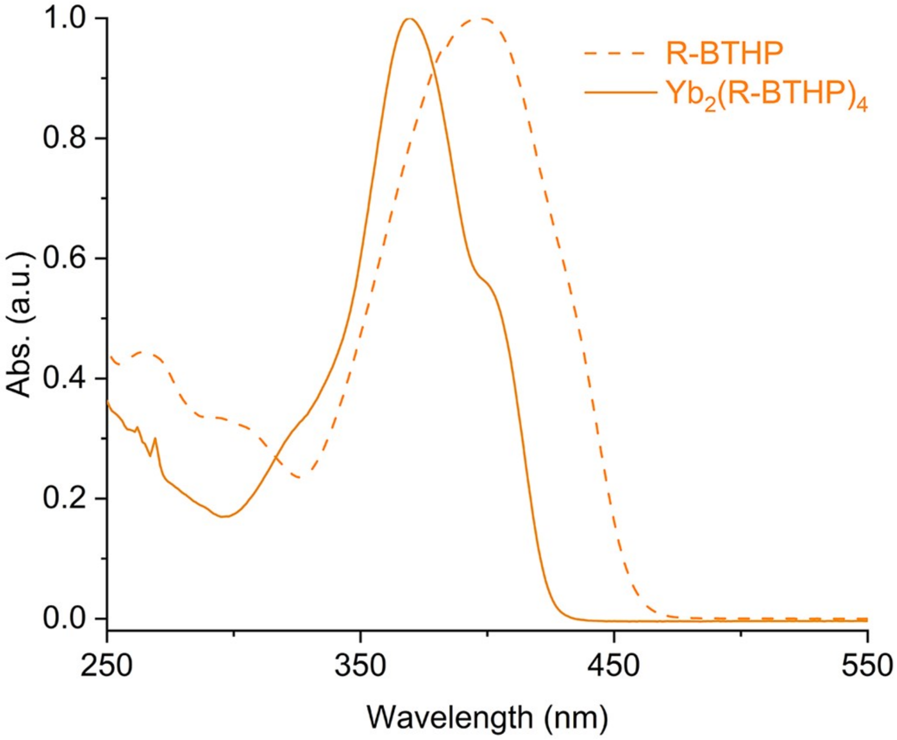

Figure S22. UV-visible absorption spectra of ligand R-BTHP ($c = 2.0 \times 10^{-5}$ M) and Yb_2(R-BTHP)$_4$ ($c = 5.0 \times 10^{-6}$ M) in THF.

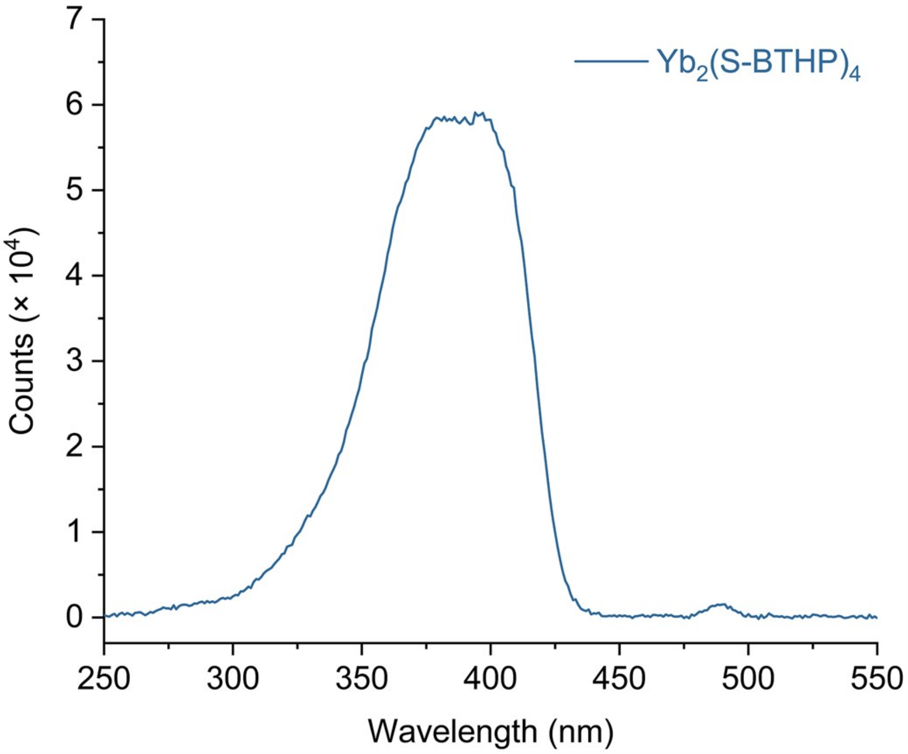

Figure S23. Excitation spectrum of Yb_2(S-BTHP)$_4$ in THF ($c = 5.0 \times 10^{-6}$ M).

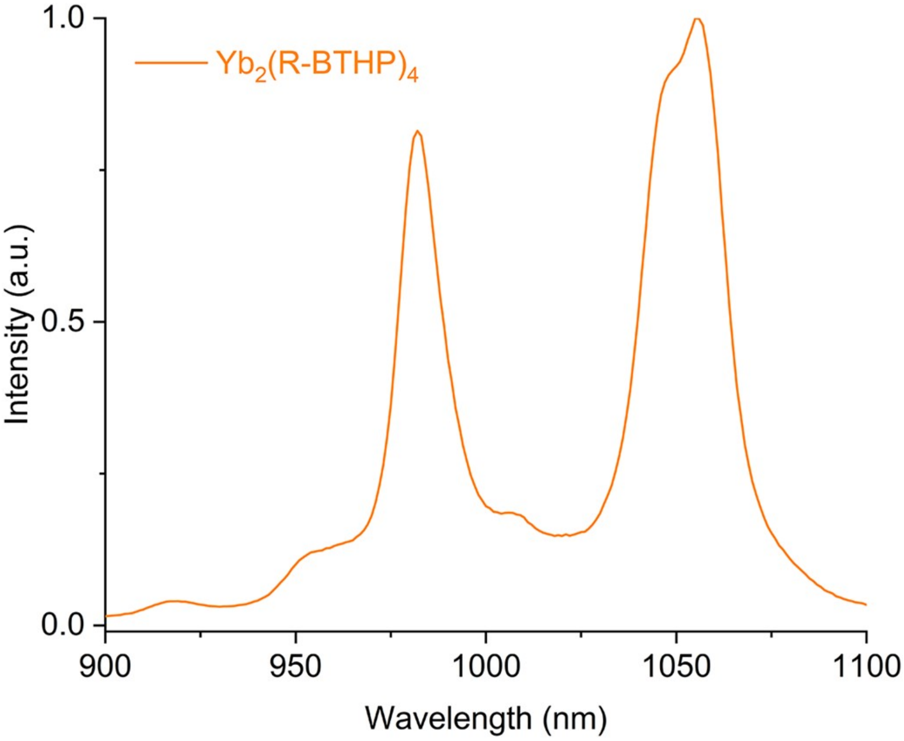

Figure S24. Emission spectrum of Yb_2(R-BTHP)$_4$ in THF ($c = 5.0 \times 10^{-6}$ M).

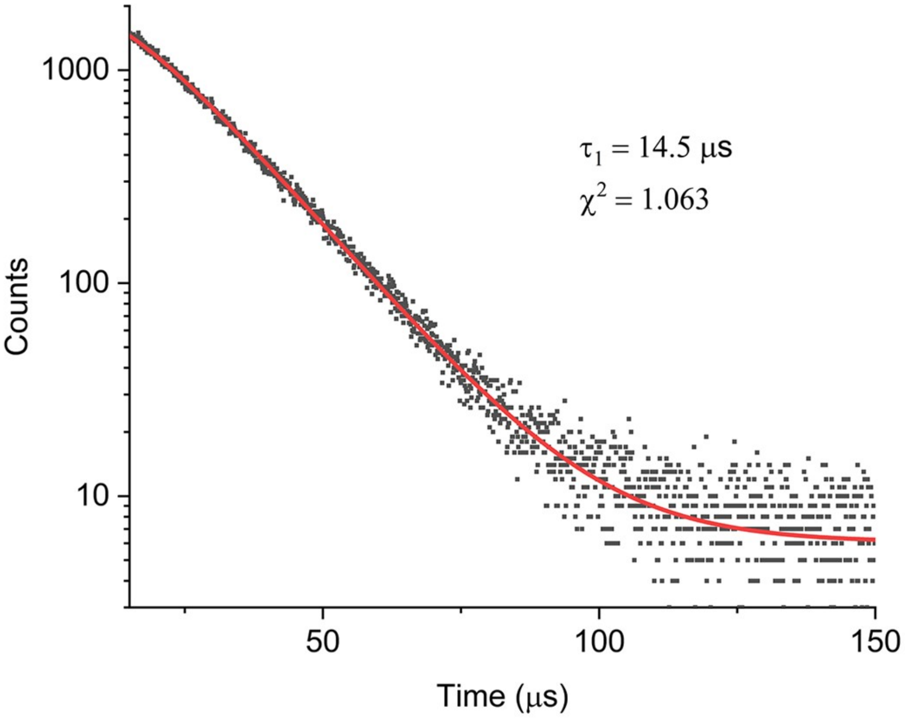

Figure S25. Luminescence decay curve of Yb_2(S-BTHP)$_4$ in THF ($c = 5.0 \times 10^{-6}$ M) monitored at 980 nm.

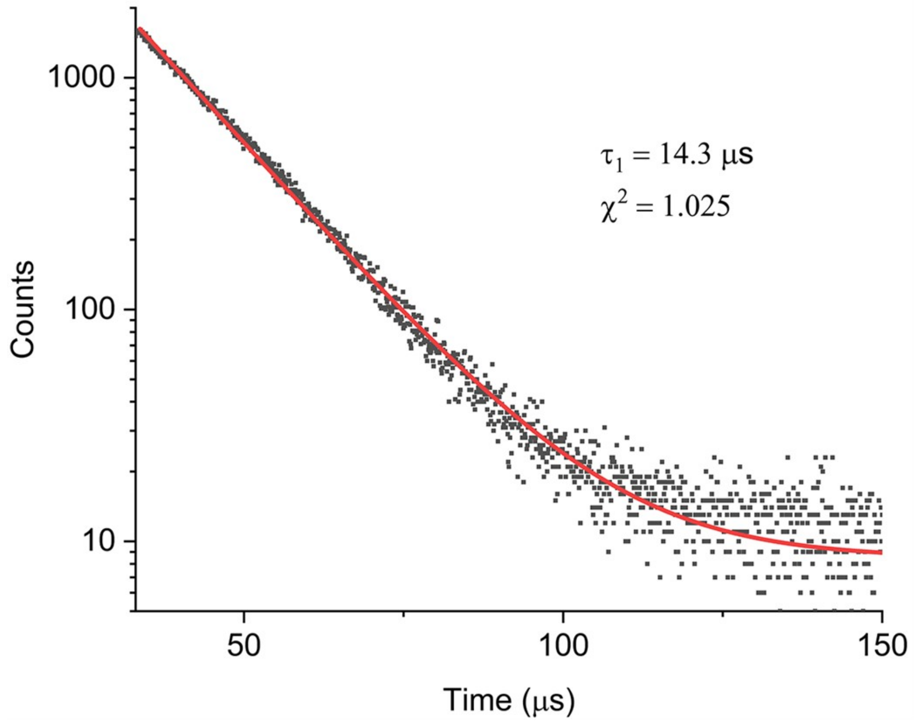

Figure S26. Luminescence decay curve of Yb_2(R-BTHP)$_4$ in THF ($c = 5.0 \times 10^{-6}$ M) monitored at 980 nm.

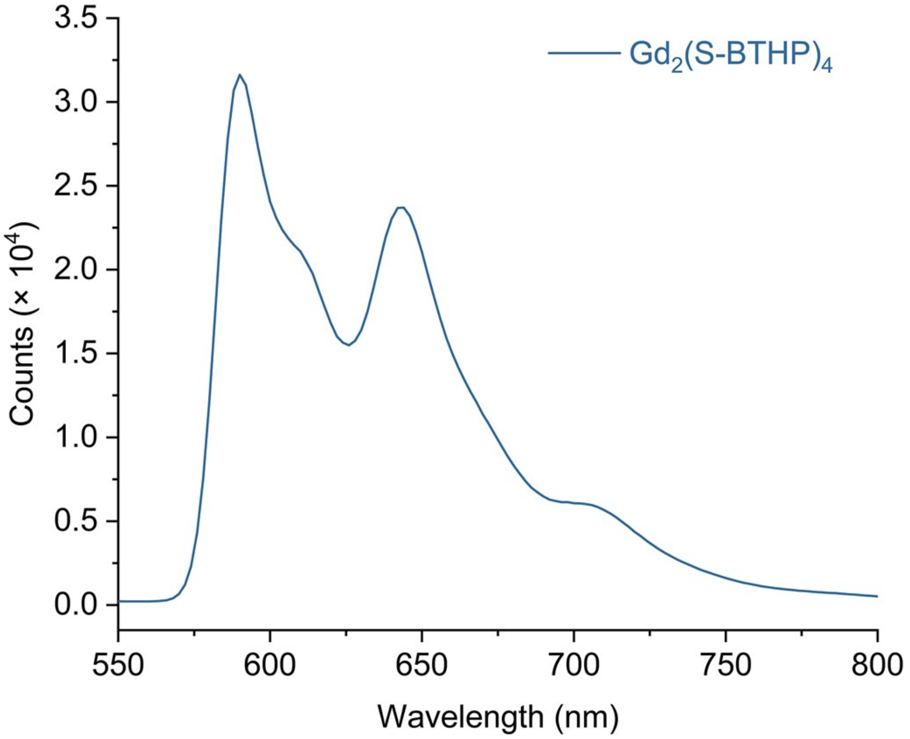

Figure S27. Phosphorescence emission spectrum of Gd_2(S-BTHP)$_4$ in THF.

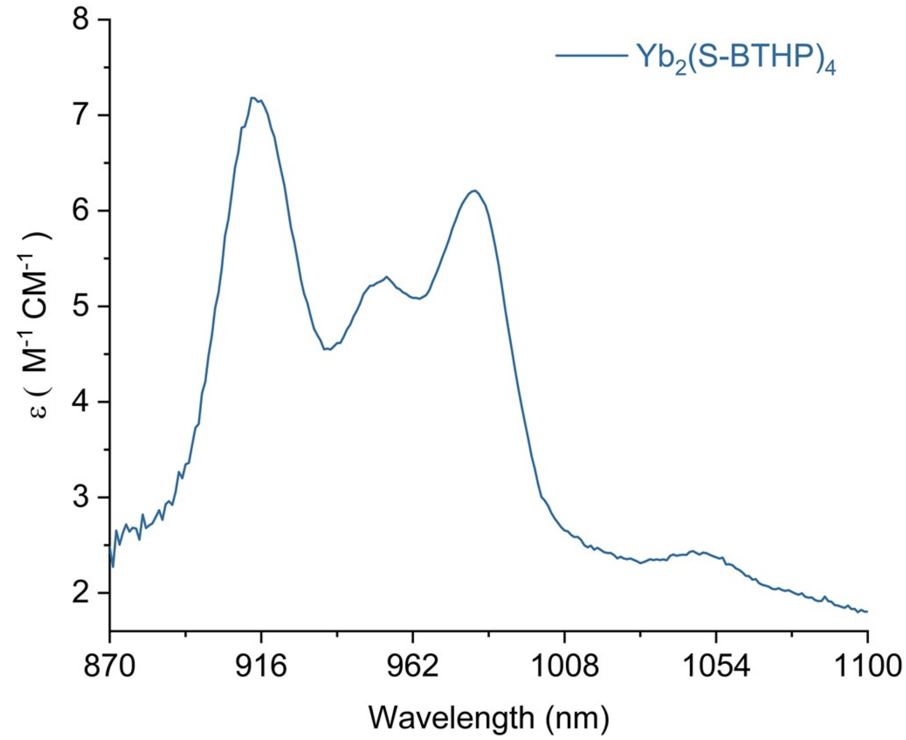

Figure S28. Near-infrared spectrum of f-f absorption transition for Yb$_2$(S-BTHP)$_4$ in THF.

Table S1. Radiative (k_r) and Nonradiative (k_{nr}) Decay Rates, Observed luminescence lifetime of Yb^{3+} (τobs), Intrinsic quantum yield (Φ_{Ln}), Sensitization efficiency (η_{sens}), and Overall quantum yield ($\Phi_{overall}$). Error in τ_{obs}: ±0.05 ms; 10% relative error in the other values; λ_{ex} = 395 nm. g_{lum} values for $^2F_{5/2} \rightarrow {}^2F_{7/2}$ of Yb^{3+} ion.

Complexes	k_r (s^{-1})	k_{nr} (s^{-1})	τ_{obs} (μs)	Φ_{Ln} (%)	η_{sens} (%)	$\Phi_{overall}$ (%)	g_{lum} $^2F_{5/2} \rightarrow {}^2F_{7/2}$	
							$g_{lum-980}$	$g_{lum-1050}$
Yb$_2$(S-BTHP)$_4$	4476	6.4×10^4	14.5	6.5	25.5	1.66	0.81	-0.11
Yb$_2$(R-BTHP)$_4$	4476	6.5×10^4	14.3	6.4	25.7	1.67	-0.80	0.12

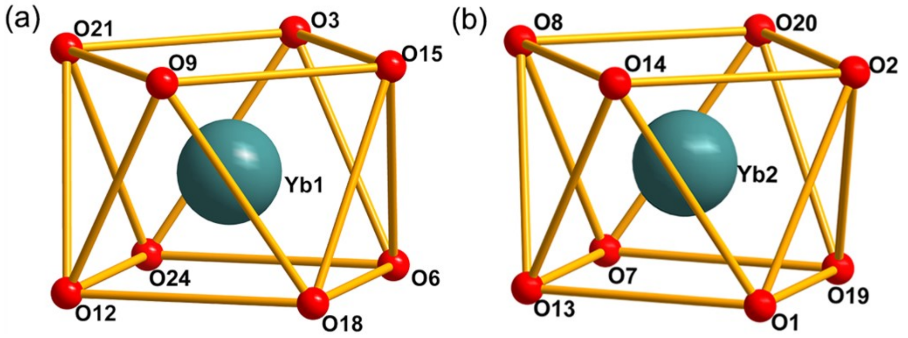

Figure S29. Coordination polyhedra of (a) Yb$_2$(S-BTHP)$_4$ (Yb1); (b) Yb$_2$(S-BTHP)$_4$ (Yb2).

Table S2. Shape analysis of ytterbium complex using SHAPE 2.1 software.

Complex	Square antiprism	Triangular dodecahedron	Biaugmented trigonal prism
$(Yb)_2(S\text{-}BTHP)_4$ (Yb1)	0.179	2.358	2.070
$(Yb)_2(S\text{-}BTHP)_4$ (Yb2)	0.230	2.302	2..098

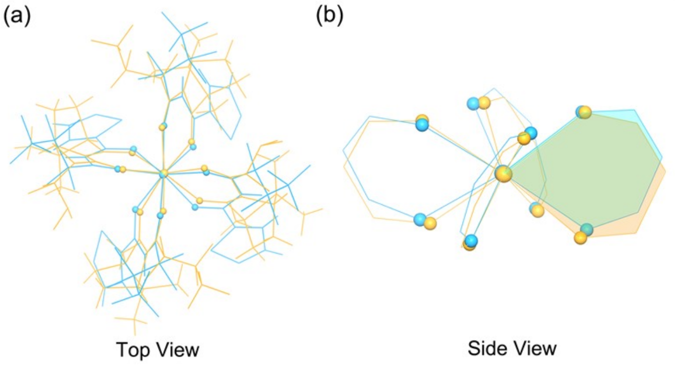

Figure S30. The crystallographic structure of first coordination sphere around Yb ion of $Yb_2(S\text{-}BTHP)_4$ (blue) over the structure of $CsYb(hfbc)_4$ (yellow).

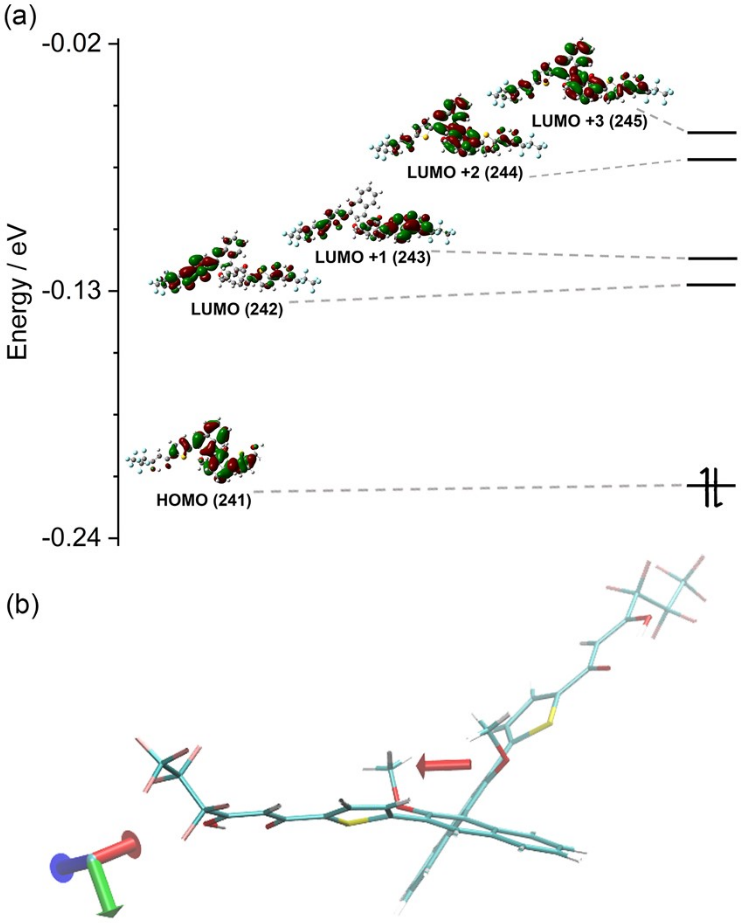

Figure S31. (a) the electronic structure of the chromophore (ground and excited states) and (b) the calculated transition dipole of ligand.

3. X-ray Crystallography

Table S3. Crystal data for the complex.

	(TMA)(H_3O)[Yb_2(S-BTHP)$_4$]
CCDC Number	2222063
Empirical formula	$C_{172}H_{103}F_{56}NO_{25}S_8Yb_2$
Formula weight	4250.11
Color	Yellow
Crystal System	tetragonal
Space group	*P4*
a (Å)	21.2823 (14)
b (Å)	21.2823(14)
c (Å)	25.490(2)
α (deg)	90
β (deg)	90
γ (deg)	90
V (Å^3)	11545.3(18)
Z	2
ρ (g cm^3)	1.223
μ (mm^{-1})	0.974
F (000)	4228
R_1,[$I > 2\sigma(I)$]	0.0512
wR_2,[$I>2\sigma(I)$]	0.1277
R_1, (all data)	0.0820
wR_2, (all date)	0.1556
GOF on F^2	1.095